Recognition of mixed-sequence DNA targets using spermine-modified Invader probes

Shiva P. Adhikari, Raymond G. Emehiser, Saswata Karmakar, and Patrick J. Hrdlicka*

Department of Chemistry, University of Idaho, Moscow, ID-83844, USA

E-mail: hrdlicka@uidaho.edu

Electronic Supplementary Information

Protocol - Synthesis and purification of ONs. Modified oligodeoxyribonucleotides (ONs) were synthesized on a computer-controlled DNA synthesizer (0.2 µmol scale) using long-chain alkyl amine-controlled pore glass (LCAA-CPG) solid support with a pore size of 500 Å. The corresponding DMTr-protected phosphoramidite of monomer **X** was prepared as previously described[S1] and incorporated into ONs via hand-couplings (0.05 M in anhydrous acetonitrile; ~50-fold molar excess) using 0.01 M 4,5-dicyanoimidazole in anhydrous acetonitrile as the activator (15 min) and 0.02 M iodine in THF//H_2O/pyridine for extended oxidation (45 s). The DMTr-protected phosphoramidite of the spermine linker was obtained from a commercial source (Glen Research - https://www.glenresearch.com/spermine-phosphoramidite.html) and incorporated into ONs via hand-couplings using the abovementioned approach (3 min). Following synthesis, the columns were treated with 10% diethylamine in acetonitrile (5 min, room temperature) and rinsed with additional acetonitrile to remove the cyanoethyl protecting groups of the spermine monomers as recommended by the vendor to prevent acrylonitrile addition to the spermine units.[S2] Subsequent treatment with 32% aq. ammonia (55 °C, 17 h) facilitated global deprotection and cleavage from the solid support. DMTr-protected ONs were purified via ion-pair reverse phase HPLC (XTerra MS C18 column: 0.05 M aq. triethyl ammonium acetate - acetonitrile gradient) and detritylated (80% aq. AcOH, 20 min) and precipitated (NaOAc, $NaClO_4$, acetone, -18 °C, 16 h). The purity of the ONs was established using analytical HPLC (>85% purity), whereas the identity was verified by MALDI-MS (using 2,4,6-trihydroxyacetophenone as a matrix) or ESI-MS (modified ONs were dissolved in 2.5 M acetic acid, 25 mM imidazole and 25 mM piperidine in 80% aq. acetonitrile)[S3] recorded on a Quadrupole Time-of-Flight (Q-TOF) mass spectrometer (Table S1). Raw ESI-signal peaks were deconvoluted using the Max Ent software provided with the spectrometer to obtain molecular ion peaks.

Table S1. MS data of ONs used in this study.[a]

ON	Sequence	Calculated *m*/*z* $(M+H)^+$	Observed *m*/*z* $(M+H)^+$
1	5'-GGTA**X**A**X**ATAGGC-3'	4445.5	4447.8
2	3'-CCATA**X**A**X**ATCCG-5'	4325.5	4326.9
3	5'-GG-**S**-TA**X**A**X**ATAGGC-3'	4855.5	4860.5
4	3'-CC-**S**-ATA**X**A**X**ATCCG-5'	4735.5	4735.1
3C	5'-GG-**S**-TATATATAGGC-3'	4423.0	4428.4
4C	3'-CC-**S**-ATATATATCCG-5'	4303.0	4302.0
7	5'-GG-**S**-TA**X**A**X**ATAG-**S**-GC-3'	5265.5	5268.8

[a] MALDI-MS was used to determine *m*/*z* for **ON1**, **ON2**, **ON4** and **ON4C**, whereas ESI-MS was used to determine *m*/*z* for **ON3**, **ON3C** and **ON7**.

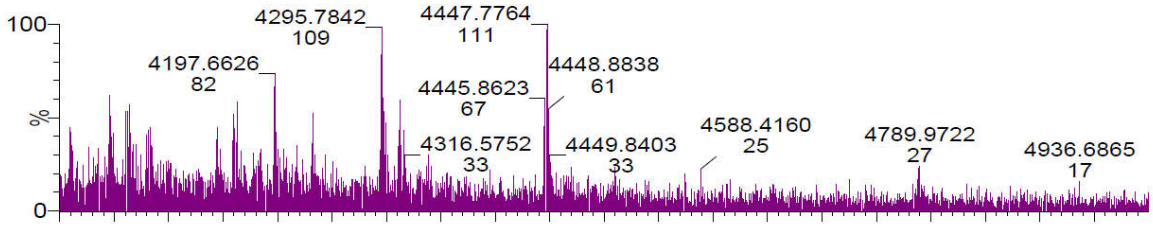

Figure S1. MALDI-MS spectrum of **ON1**.

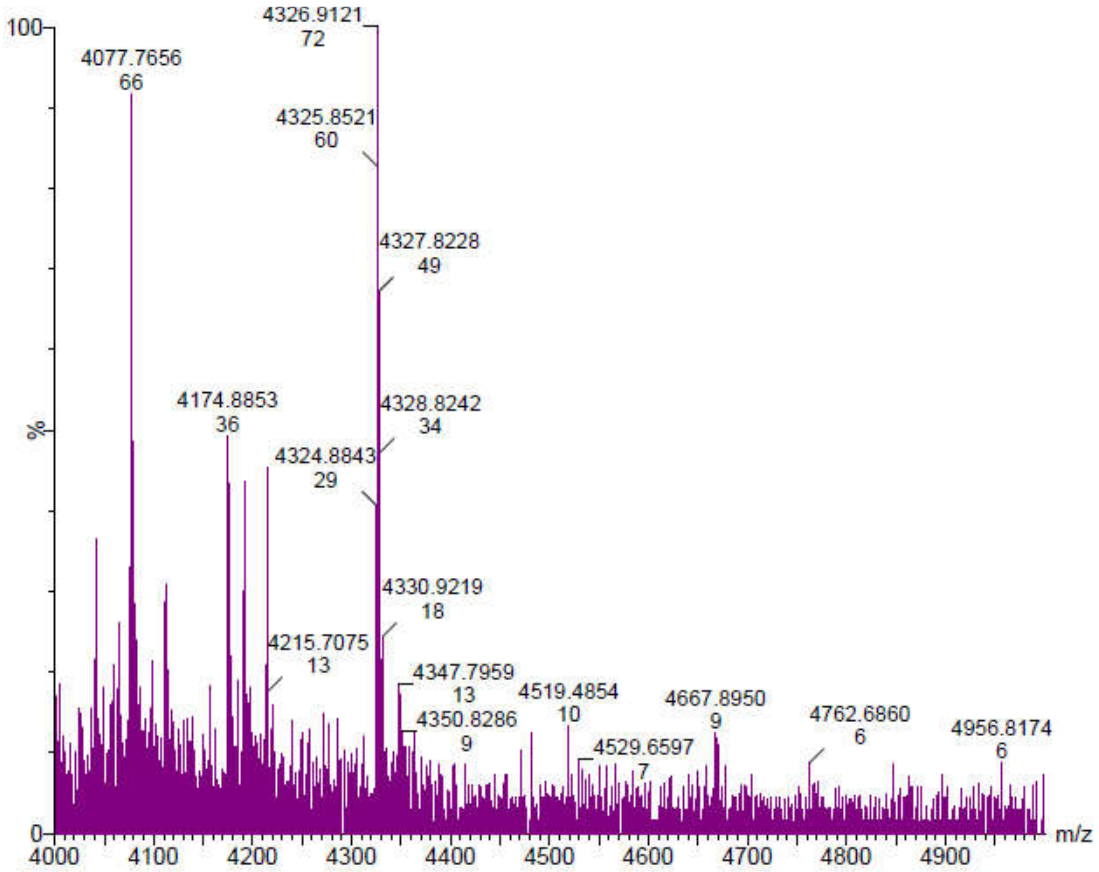

Figure S2. MALDI-MS spectrum of **ON2**.

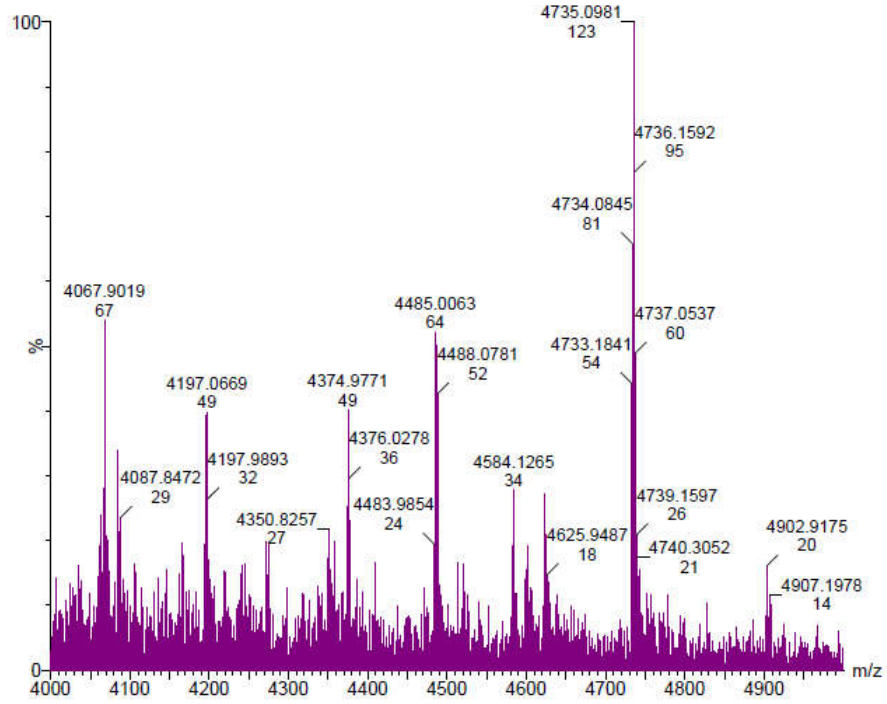

Figure S3. MALDI-MS spectrum of **ON4**.

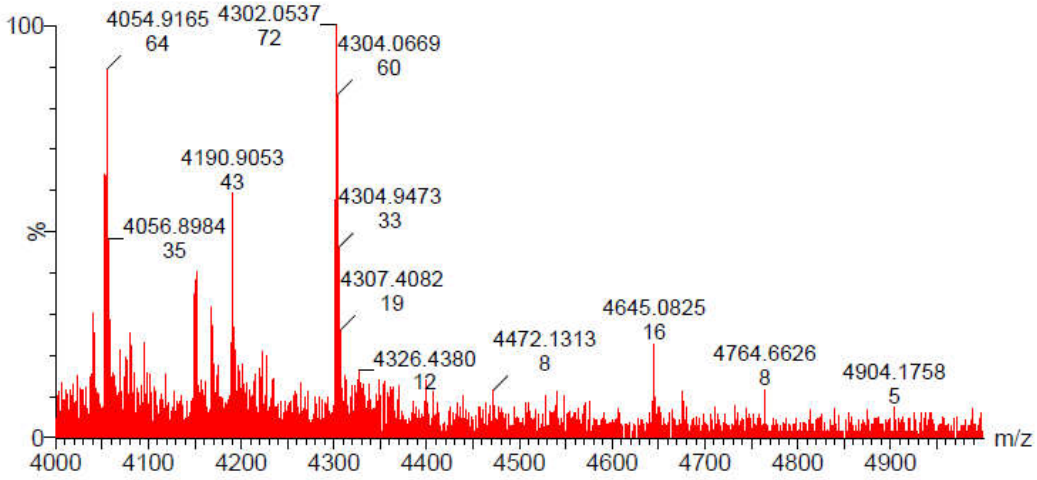

Figure S4. MALDI-MS spectrum of **ON4c**.

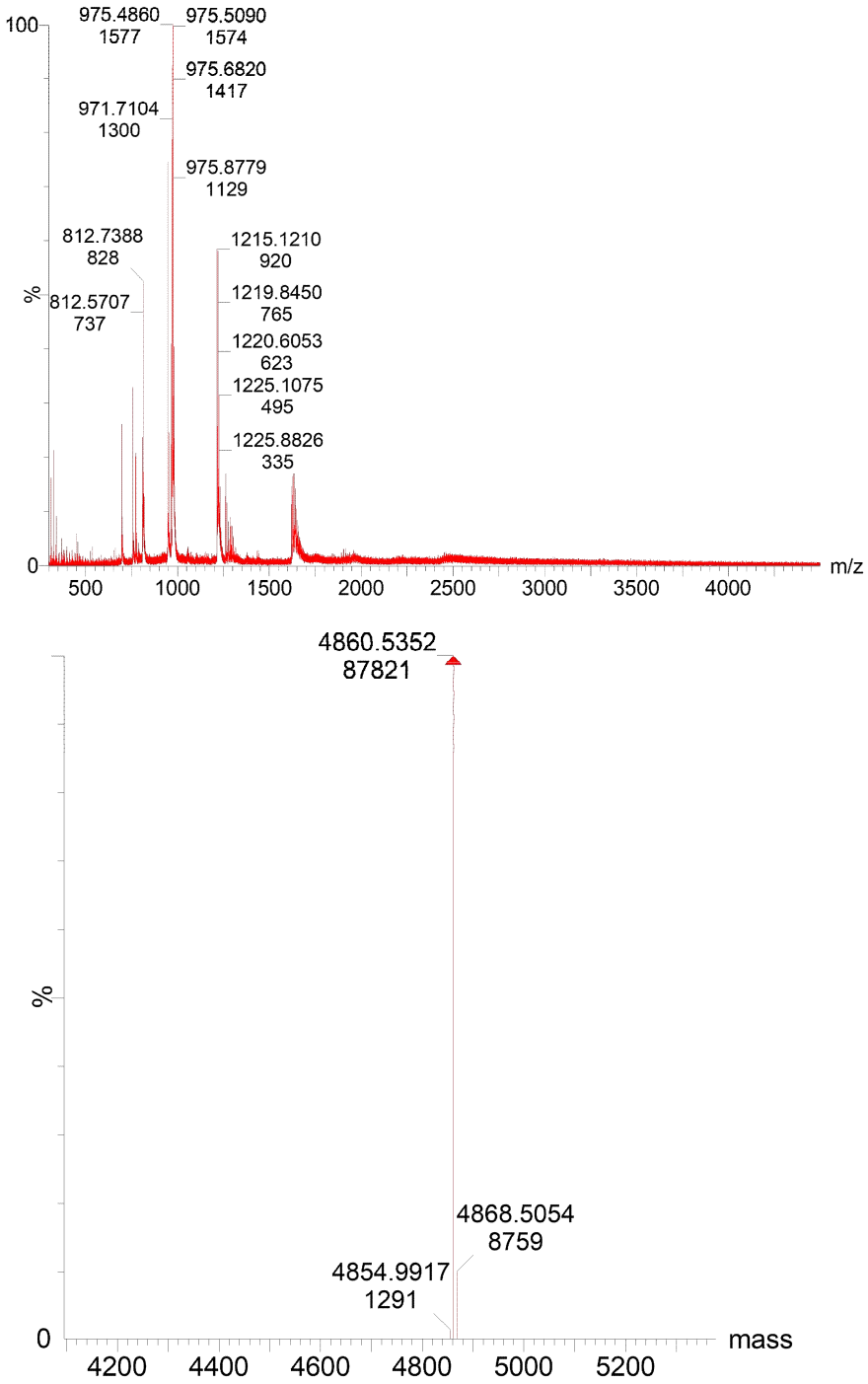

Figure S5. Unprocessed (upper panel) and deconvoluted (lower panel) ESI-MS spectrum of **ON3**.

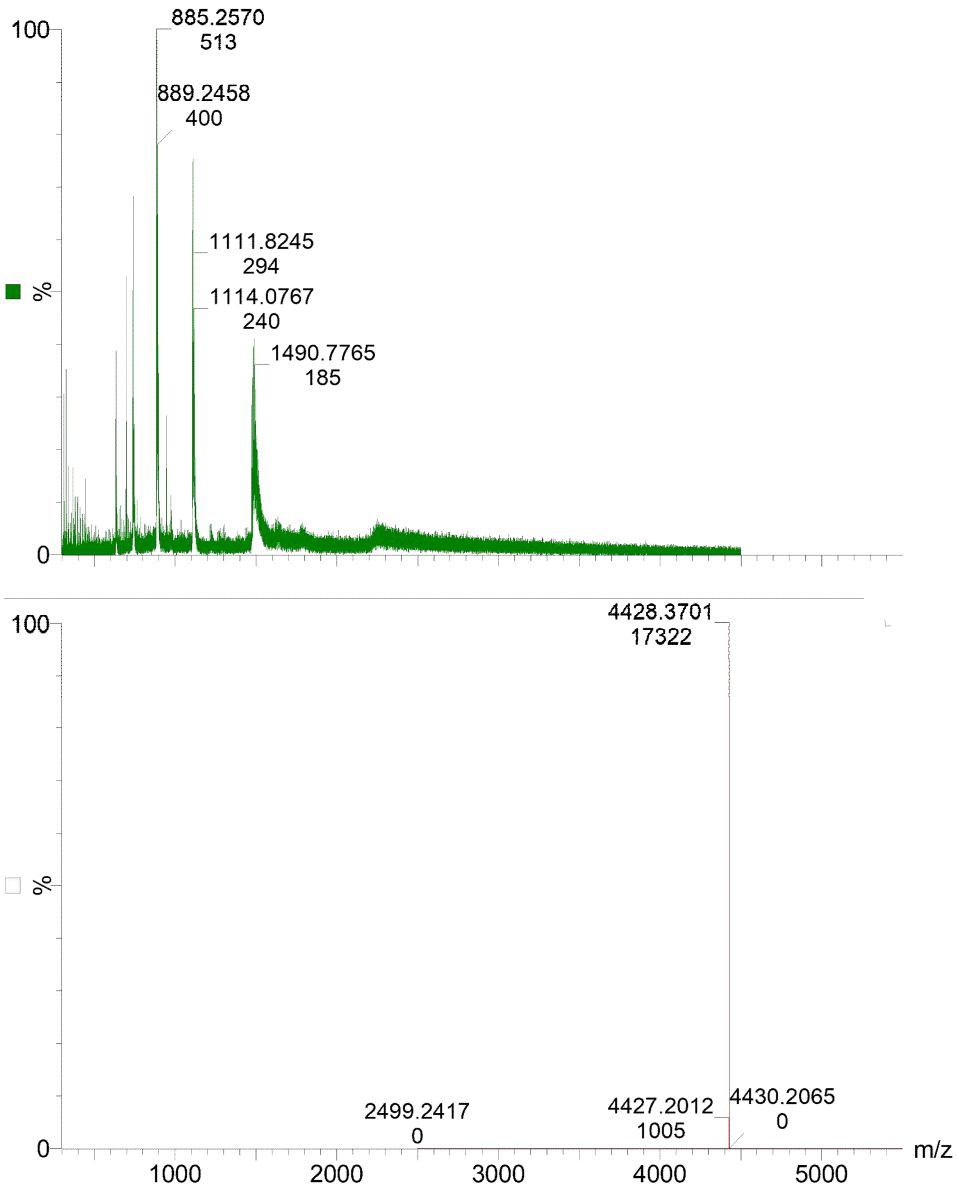

Figure S6. Unprocessed (upper panel) and deconvoluted (lower panel) ESI-MS spectrum of **ON3c**.

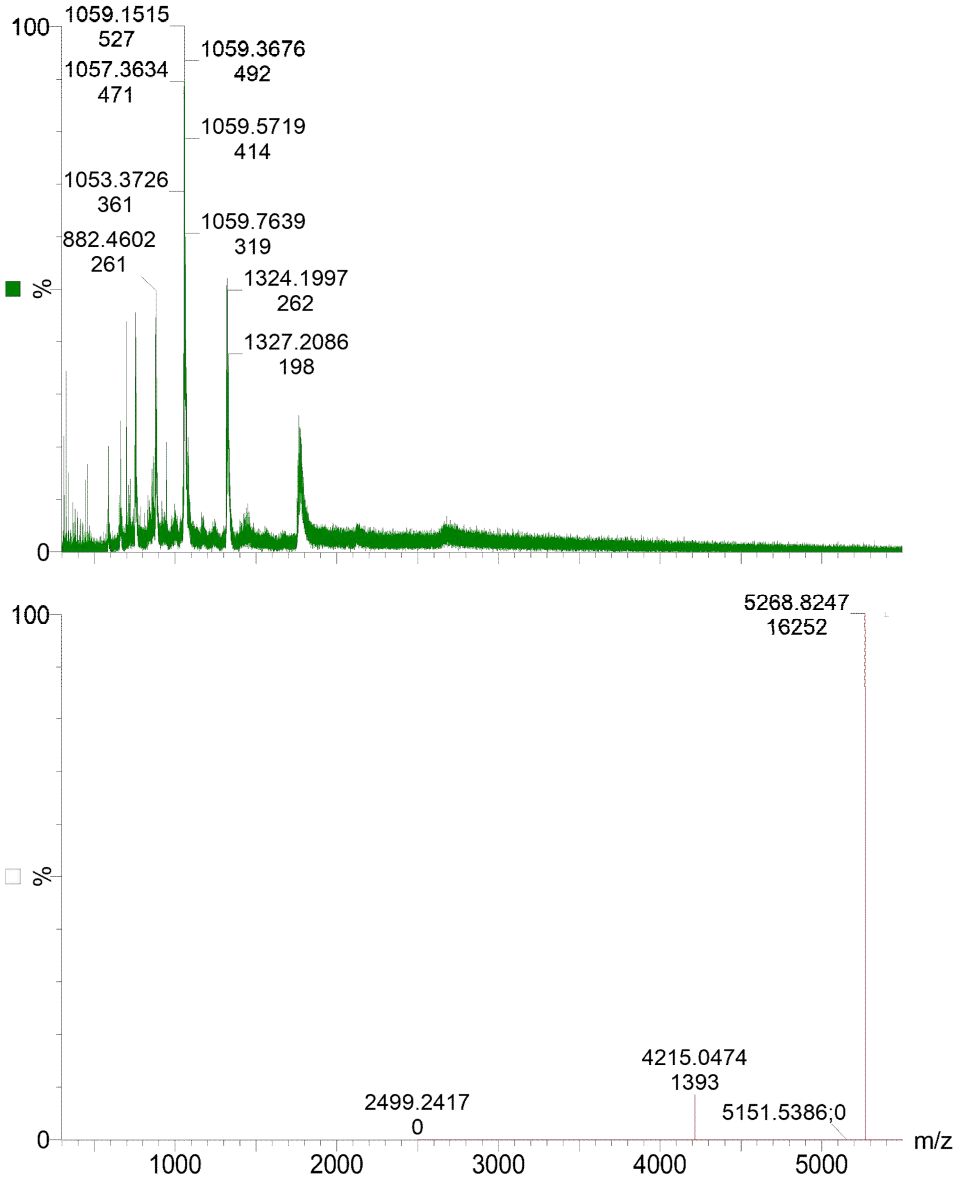

Figure S7. Unprocessed (upper panel) and deconvoluted (lower panel) ESI-MS spectrum of **ON7**.

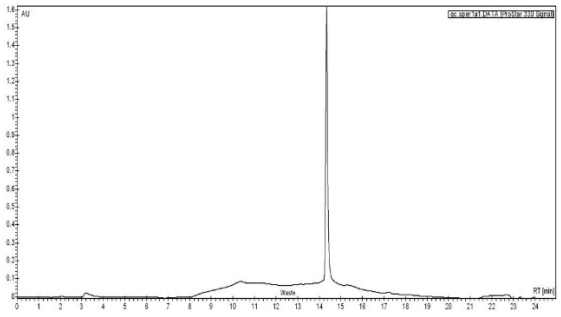

ON1

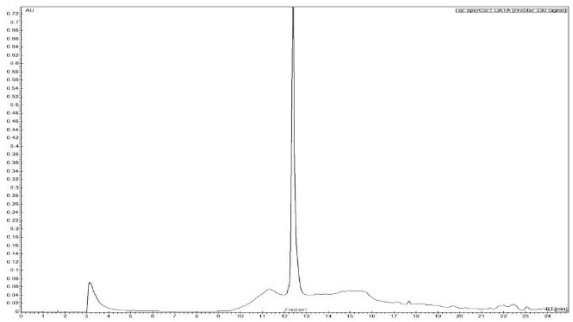

ON3c

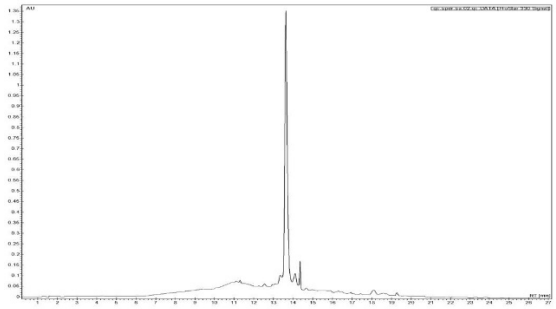

ON2

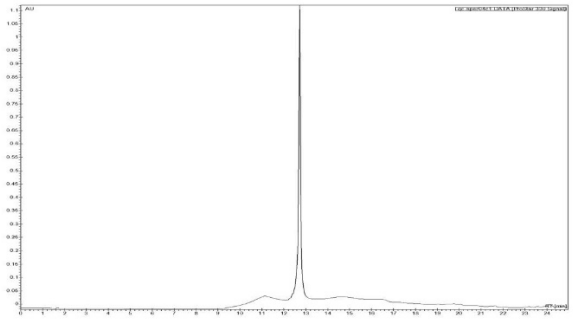

ON4c

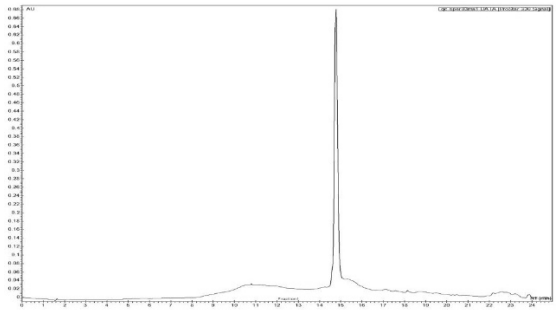

ON3

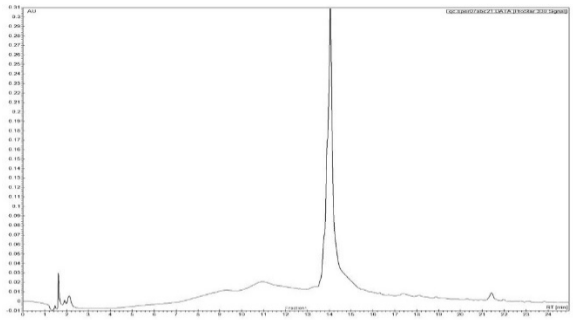

ON7

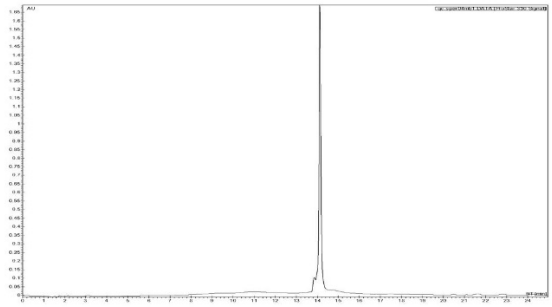

ON4

Figure S8. HPLC traces for modified ONs used in this study.

Protocol - thermal denaturation experiments. The concentrations of ONs were estimated using the following extinction coefficients (OD_{260}/μmol): G (12.01), A (15.20), T (8.40), C (7.05) and pyrene (22.4)[S4]. Thermal denaturation temperatures (T_ms) of duplexes (1 μM final concentration of each strand) were measured on a Cary 100 UV/VIS spectrophotometer equipped with a 12-cell Peltier temperature controller and determined as the maximum of the first derivative of thermal denaturation curves (A_{260} vs. T) recorded in medium salt buffer (T_m buffer: 100 mM NaCl, 0.2 mM EDTA, and pH 7.0 adjusted with 10 mM Na_2HPO_4 and 5 mM Na_2HPO_4). Strands were mixed in quartz optical cells with a path length of 1.0 cm and annealed by heating to 85 °C (2 min), followed by cooling to the starting temperature of the experiment. A temperature range from 3 °C (low salt) or 10 °C (medium salt) to at least 20 °C above the duplex T_m was used, with T_ms determined as the average of two experiments within ±1.0 °C. A temperature ramp of 1 °C/min was used in all experiments.

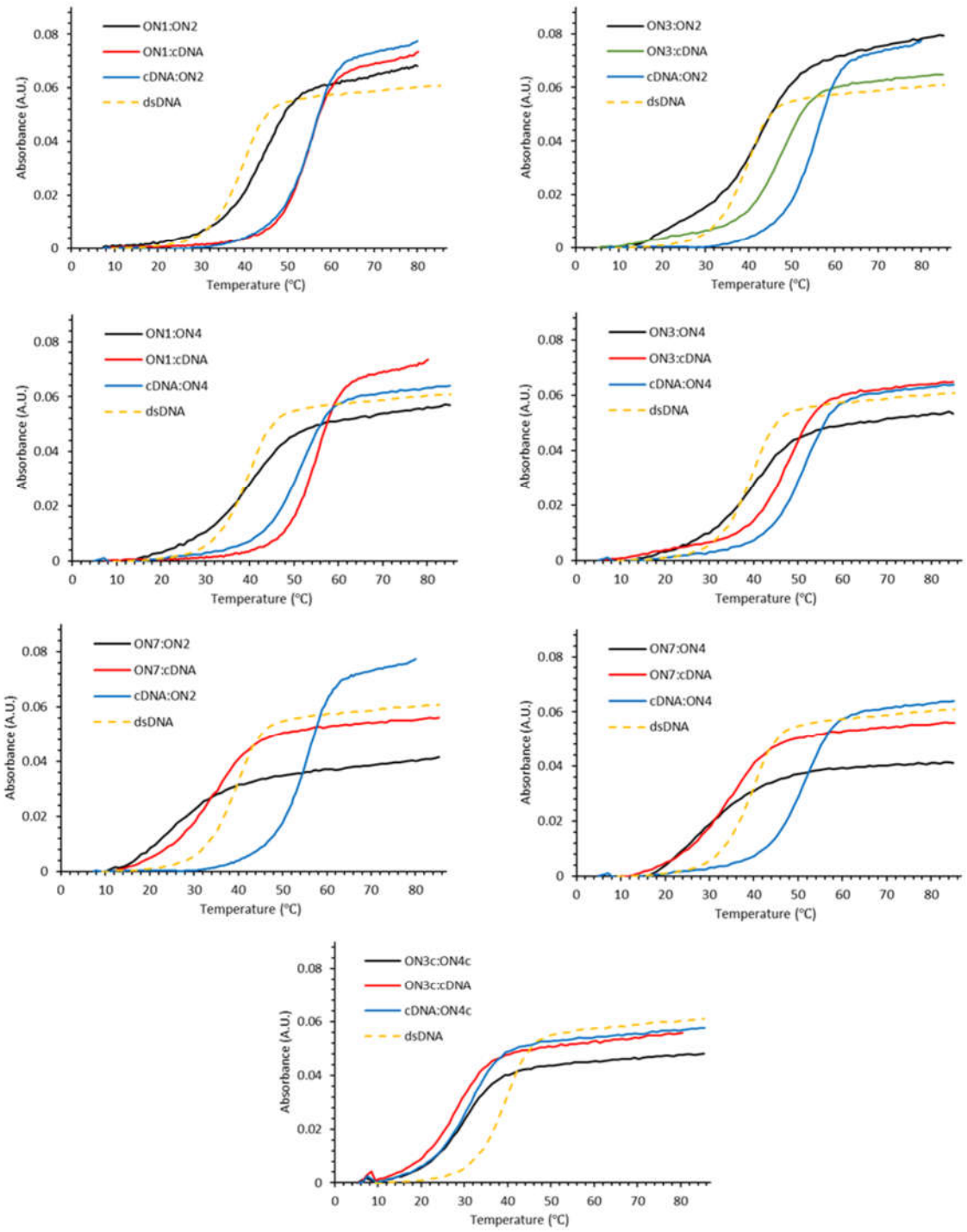

Figure S9. Representative thermal denaturation curves of Invader probes, duplexes between individual probe strands and cDNA, and unmodified reference duplexes recorded in *medium salt* buffer. Experimental conditions are described in Table 1.

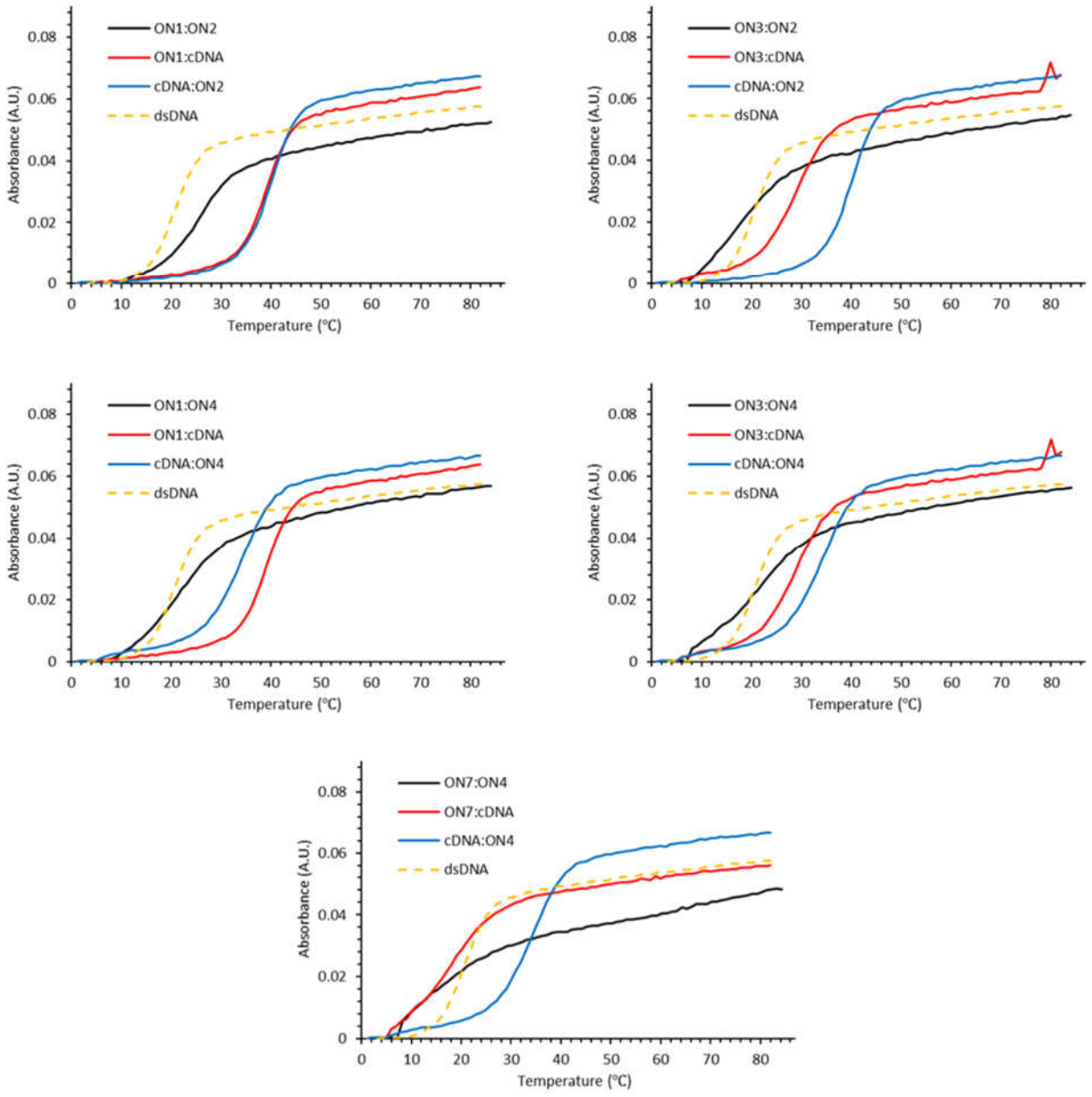

Figure S10. Representative thermal denaturation curves of Invader probes, duplexes between individual probe strands and cDNA, and unmodified reference duplexes recorded in *low salt* buffer. Experimental conditions are described in Table S2.

Trends of T_ms determined at low ionic strength. The T_ms of all duplexes are substantially lower at low ionic strength ([Na^+] = 10 mM, Table S2) than at medium ionic strength ([Na^+] = 110 mM, Table 1), as lower salt concentrations increase the electrostatic repulsion between polyanionic strands. Interestingly, probe duplexes are 2.5-6 °C more destabilized at low vis-à-vis medium ionic strength relative to the unmodified DNA reference duplex (e.g., ΔT_m for **ON1**:**ON2** = +3.5 °C vs +7.5 °C at low and medium strength, respectively), whereas duplexes between individual probe strands and cDNA duplexes are 0-3 °C more stable relative to the unmodified DNA reference duplex (e.g., ΔT_m for **ON1**:cDNA = +18 °C at either condition). Consequently, the probes are more strongly activated for dsDNA-recognition at low salt conditions (i.e., *TA* values are increased by 4.5-8.0 °C). The decrease in ΔT_m seen for probes at low ionic strength appears, in most part, to be an effect of the +1 interstrand zipper arrangements of **X** monomers rather than the spermine bulges. Thus, the relative effect of the change in salt concentration, calculated as ΔT_m (low salt) - ΔT_m (medium salt), is -2.5 °C for Invader probe **ON3**:**ON4** with two opposing spermine monomers and approximately -5.5 °C for single bulge Invader probes **ON3**:**ON2** and **ON1**:**ON4** and -4.0 °C for conventional Invader probe **ON1**:**ON2**. Evidently, **ON3**:**ON4** is far more stable than would be expected based on the T_m's of **ON3**:**ON2** and **ON1**:**ON4** suggesting that the overriding effect of the spermine bulges is a reduction of the net negative charge of the strands. We speculate that opposing spermine bulges are too far from each other to exert destabilizing electrostatic interactions (a fully extended protonated spermine residue spans a distance equivalent to ~5 base pairs;[S5] an internal spermine bulge would, therefore, be expected to project a distance of up to 2-3 base pairs out from a duplex). We note that prior work, in which 5'-spermine-conjugated ONs were hybridized with complementary 3'-spermine-conjugated ONs, showed that opposing terminal spermine residues only have a limited effect on each other.[S5]

Table S2. T_ms of probe duplexes and duplexes between individual probe strands and cDNA determined at *low ionic* strengths, as well as, thermal advantages (TAs) of probes.[a]

Probe	Sequence	T_m [ΔT_m] (°C)			*TA* (°C)
		probe	upper strand vs cDNA	lower strand vs cDNA	
1:2	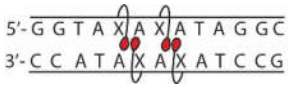	24.0 [+3.5]	38.5 [+18.0]	39.0 [+18.5]	33.0
3:2	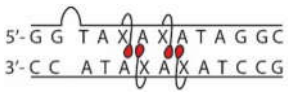	16.0 [-4.5]	31.5 [+11.0]	39.0 [+18.5]	34.0
1:4	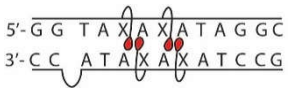	20.0 [-0.5]	38.5 [+18.0]	36.0 [+15.5]	34.0
3:4	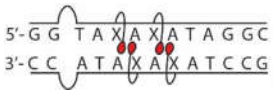	21.5 [+1.0]	31.5 [+11.0]	36.0 [+15.5]	25.5
7:4	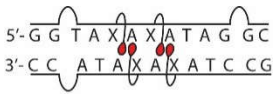	<15 [<-5.5]	21.0 [+0.5]	36.0 [+15.5]	>21.5

*ΔT_ms are calculated relative to the corresponding unmodified dsDNA (T_m = 20.5 °C). Thermal denaturation curves were recorded in low salt phosphate buffer ([Na^+] = 10 mM, pH 7.0 (NaH_2PO_4/Na_2HPO_4), [EDTA] = 0.2 mM) and each [ON] = 1.0 μM.

Protocol - electrophoretic mobility shift assay. DNA hairpins were obtained from commercial sources and were used without further purification. The DNA hairpins were DIG-labeled using the 2nd generation DIG Gel Shift Kit (Roche Applied Bioscience). Briefly, 11-digoxigenin-ddUTP was incorporated at the 3′-end of the hairpin (100 pmol) using a recombinant DNA terminal transferase. The reaction mixture was quenched through addition of EDTA (0.05 M), diluted to 68.8 nM in 2X HEPES buffer, and used without further processing. The recognition experiments were conducted essentially as previously reported.[S6] Thus, Invader probes (variable 2X concentration in water) were annealed (90 °C for 2 min, followed by cooling to room temperature) and subsequently incubated with DIG-labeled DNA hairpins (34.4 nM final concentration in 1X HEPES buffer: 50 mM HEPES, 100 mM NaCl, 5 mM $MgCl_2$, pH 7.2, 10% sucrose, 1.44 mM spermine tetrahydrochloride) at either 8 °C ± 2 °C, 25 °C ± 2 °C, or 37 °C ± 2 °C for 17 hours. One microliter of loading dye (6X) was added and the reaction mixtures were loaded onto 12% non-denaturing TBE-PAGE gels (45 mM tris-borate, 1 mM EDTA; acrylamide:bisacrylamide (19:1)). Electrophoresis was performed using constant voltage (70 V) at ~4 °C for 1.5 h. Bands were blotted onto positively charged nylon membranes (100 V, 30 min, ~4 °C) and cross-linked through exposure to UV light (254 nm, 5 × 15 W bulbs, 3 min). Membranes were incubated with anti-digoxigenin alkaline phosphatase F_{ab} fragments as recommended by the manufacturer and transferred to a hybridization jacket. Membranes were incubated with CSPD for 10 min at 37 °C, and chemiluminescence from the formed product was captured on X-ray films. Digital images of developed X-ray films were obtained using a Fluor-S MultiImager and quantified using appropriate software (Quantity One). The percentage of dsDNA recognition was calculated as the intensity of the recognition complex band relative to the total intensity of all bands. An average of three independent experiments is reported along with standard deviations (±). Non-linear

regression was used to fit data points from dose-response experiments. A script written for the "Solver" module in Microsoft Office Excel,[S7] was used to fit the following equation to the data points: $y = C + A\ (1 - e^{-kt})$ where C, A and k are constants. The resulting equation was used to calculate C_{50} values by setting $y = 50$ and solving for t.

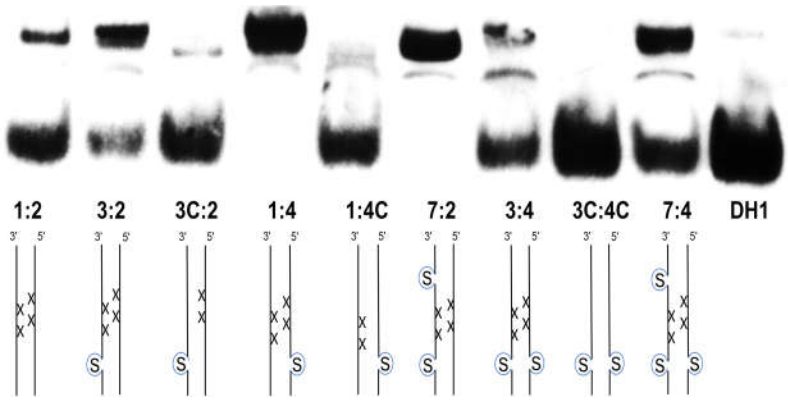

Figure S11. Representative electrophoretogram depicting recognition of model dsDNA target **DH1** using 100-fold molar excess (3.44 μM) of different probes at 8 °C. Experimental conditions are otherwise as described in Figure 2.

Table S3. Levels of recognition of DNA hairpin **DH1** using a 200-fold molar excess (at 25 °C) or 100-fold molar excess (at 8 °C) of various double-stranded probes.[a]

		Recognition (%)	
Probe	**Sequence**	**8 °C**	**25 °C**
1:2	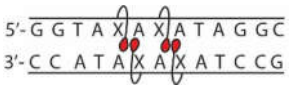	20±2	>90
3:2	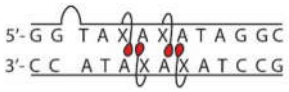	23±4	>90
1:4	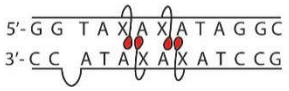	29±3	>90
3:4	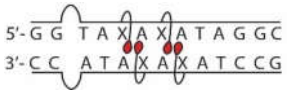	9±8	45±1
7:2	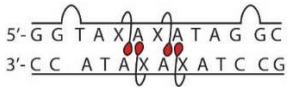	34±5	>90
7:4	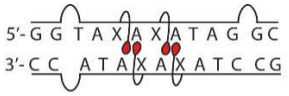	15±2	36±8
3c:4c		<5	<5
3c:2	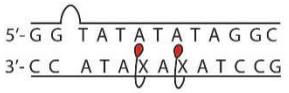	<5	11±5
1:4c	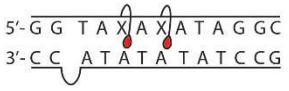	<5	21±3

[a] Experiments were performed in triplicate. Conditions are described in Figure 2.

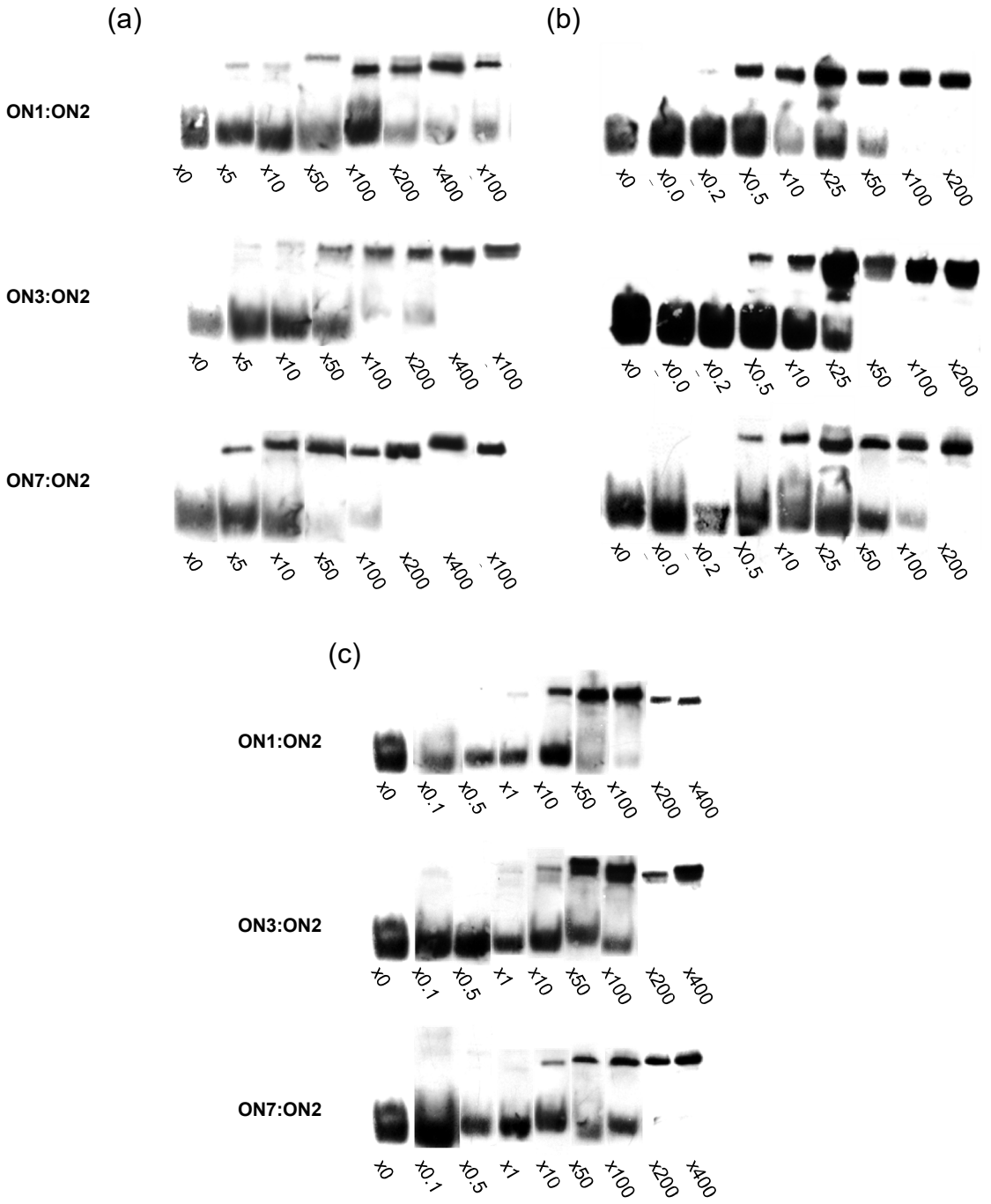

Figure S12. Representative electrophoretograms illustrating dose-response experiment between dsDNA target **DH1** (34.4 nmol) using a variable molar excess of Invader probes **ON1**:**ON2**, **ON3**:**ON2**, and **ON7**:**ON2** at a) 8 °C, b) 25 °C, and c) 37 °C. Experimental conditions are otherwise as described in Figure 2.

Table S4. Seqeuences and T_ms of DNA hairpins used in this study.[a]

DH	Sequence	T_m (°C)
1		58.5
2		60.5
3		63.5
4		63.0
5		60.0
6		62.5
7		62.5

[a] For experimental conditions, see Table 1. Data previously published in reference S6.

Supplementary references.

S1) S. Karmakar, B. A. Anderson, R. L. Rathje, S. Andersen, T. B. Jensen, P. Nielsen and P. J. Hrdlicka, *J. Org. Chem.*, 2011, **76**, 7119-7131.

S2) Glen Report 24.11: https://www.glenresearch.com/reports/gr24-11 - accessed July 30, 2019.

S3) D. C. Muddiman, X. Cheng, H. R. Udseth and R. D. Smith, *J. Am. Soc. Mass Spectrom.*, 1996, **7**, 697-706.

S4) N. N. Dioubankova, A. D. Malakhov, D. A. Stetsenko, M. J. Gait, P. E. Volynsky, R. G. Efremov and V. A. Korshun, *ChemBioChem*, 2003, **4**, 841-847.

S5) R. Noir, M. Kotera, B. Pons, J.-S. Remy and J.-P. Behr, *J. Am. Chem. Soc.*, 2008, **130**, 13500-13505.

S6) D. C. Guenther, G. H. Anderson, S. Karmakar, B. A. Anderson, B. A. Didion, W. Guo, J. P. Verstegen and P. J. Hrdlicka, *Chem. Sci.*, 2015, **6**, 5006-5015.

S7) A. M. Brown, *Comput. Methods Prog. Biol.*, 2001, **65**, 191-200.